**Reply to Anonymous Referee #4**

We thank Anonymous Referee #4 for the valuable comments on our manuscript. Here we provide point-to-point responses to the Referees' comments. For clarity, the Referees' comments are marked in black, authors' responses are marked in **blue**, and changes in the manuscript are marked in **red**.

This investigated the chemical compositions and properties of marine aerosols over the Bohai Sea and Yellow Sea. This work is generally well-written and within the scope of ACP. I support the publication once the following comments are addressed.

1. For the PMF source apportionment analysis, I'm confused by the statements in lines 346-350. Have the authors investigated the uncertainty of your PMF results? This is needed before discussion based on the results. Sometimes, terrestrial sources and anthropogenic pollutants occur at the same time. Have the authors check the collinearity between sources (e.g., secondary inorganic aerosols, combustion, secondary organic aerosols, dust)?

**Author reply:**

Concerning the statement at lines 346–350, our original idea was to express that combining TSP and $PM_{2.5}$ samples for PMF source apportionment yields better results than conducting source apportionment separately for TSP and $PM_{2.5}$, because the larger the dataset, the more reliable the PMF parsing results are. We have rewritten the sentence in the manuscript as follows (Page 14, Line 362–363):

In order to ensure that the dataset is large enough to generate more reliable results for PMF, we integrated all TSP and $PM_{2.5}$ samples into one dataset, and results are shown in Fig. 4A.

Regarding the uncertainty in the PMF results, we have added additional error estimation analysis, residual analysis, and fitting coefficients of each species in the model. Table R1 shows the two error estimation methods: Displacement (DISP) and Bootstrap (BS).

The fact that no factors swaps are observed in DISP result this indicates no significant rotational ambiguity and a relatively robust solution. BS results show that although not all of the base factors were mapped to the boot factors, matching rates of all factors are close to 100%, with only one factor having a low matching rate that still exceeds 80%. This indicates that the five–factor solution is relatively stable. The unmapped factors may be due to the combination of the high variability in the data and PMF not fitting all of the data.

We also verified the error evaluation results of the four–factor and six–factor solutions. The matching rate of each of these solutions (Table R2 and Table R3) is lower than that of the five–factor solution, and their Q(True)/Q(Robust) ratios are higher than that of the five–factor solution (Figure R1). Low Q(True)/Q(Robust) ratio is usually indicative of the reasonableness of the model results (Song et al., 2018b). Low Q(True)/Q(Robust) ratio and high matching rate indicate that five factors are more suitable than four factors. In addition, the fitting coefficients of each species in the five–factor solution are high enough (Table R4). The scaled residuals of all species in the five–factor solution are mainly within + 3 and – 3 (Figure R2), indicating that each species fits well in the model. Hence, we finally report the results of the five–factor solution.

Table R1. Results of two error estimation methods (Displacement: DISP, Bootstrap: BS) for five–factor solution.

| DISP Diagnostics | | | | | | |
|---|---|---|---|---|---|---|
| Error Code: | 0 | | | | | |
| Largest Decrease in Q: | -0.047 | | | | | |
| %dQ: | -0.0071 | | | | | |
| Swaps by Factor: | 0 | 0 | 0 | 0 | 0 | |
| BS Mapping | | | | | | |
| | Base Factor 1 | Base Factor 2 | Base Factor 3 | Base Factor 4 | Base Factor 5 | Unmapped |
| Boot Factor 1 | 96 | 0 | 2 | 1 | 1 | 0 |
| Boot Factor 2 | 0 | 98 | 0 | 0 | 0 | 2 |
| Boot Factor 3 | 1 | 0 | 99 | 0 | 0 | 0 |
| Boot Factor 4 | 1 | 3 | 3 | 89 | 3 | 1 |
| Boot Factor 5 | 0 | 0 | 0 | 0 | 100 | 0 |

Table R2. Results of two error estimation methods (Displacement: DISP, Bootstrap: BS) for four–factor solution.

| DISP Diagnostics | | | | | |
|---|---|---|---|---|---|
| Error Code: | 0 | | | | |
| Largest Decrease in Q: | -0.056 | | | | |
| %dQ: | -0.0044 | | | | |
| Swaps by Factor: | 0 | 0 | 0 | 0 | |
| BS Mapping | | | | | |
| | Base Factor 1 | Base Factor 2 | Base Factor 3 | Base Factor 4 | Unmapped |
| Boot Factor 1 | 95 | 0 | 0 | 4 | 1 |
| Boot Factor 2 | 2 | 90 | 2 | 2 | 4 |
| Boot Factor 3 | 4 | 3 | 89 | 3 | 1 |
| Boot Factor 4 | 4 | 1 | 0 | 94 | 1 |

Table R3. Results of two error estimation methods (Displacement: DISP, Bootstrap: BS) for six–factor solution.

| DISP Diagnostics | | | | | | | |
|---|---|---|---|---|---|---|---|
| Error Code: | 0 | | | | | | |
| Largest Decrease in Q: | -0.011 | | | | | | |
| %dQ: | -0.030 | | | | | | |
| Swaps by Factor: | 0 | 0 | 0 | 0 | 0 | 0 | |
| BS Mapping | | | | | | | |
| | Base Factor 1 | Base Factor 2 | Base Factor 3 | Base Factor 4 | Base Factor 5 | Base Factor 6 | Unmapped |
| Boot Factor 1 | 97 | 0 | 2 | 1 | 0 | 0 | 0 |
| Boot Factor 2 | 4 | 71 | 5 | 5 | 3 | 9 | 3 |
| Boot Factor 3 | 5 | 2 | 84 | 3 | 2 | 4 | 0 |
| Boot Factor 4 | 4 | 9 | 2 | 78 | 5 | 2 | 0 |
| Boot Factor 5 | 0 | 0 | 0 | 0 | 100 | 0 | 0 |
| Boot Factor 6 | 0 | 1 | 0 | 0 | 0 | 99 | 0 |

Table R4. Fitting results between observed concentration and predicted concentration of each species in the five–factor solutions.

| | Four–factor solution | Five–factor solution | Six–factor solution |
|---|---|---|---|
| Species | $r^2$ | $r^2$ | $r^2$ |
| Particle | 0.70 | 0.70 | 0.70 |

| | | | |
|---|---|---|---|
| OC | 0.86 | 0.94 | 0.97 |
| EC | 0.55 | 0.72 | 0.76 |
| WSOC | 0.96 | 0.97 | 0.98 |
| HULIS | 0.93 | 0.93 | 0.97 |
| SOC | 0.75 | 0.98 | 0.97 |
| $Na^+$ | 0.97 | 0.98 | 0.99 |
| $NH_4^+$ | 0.98 | 0.98 | 0.98 |
| $K^+$ | 0.83 | 0.82 | 0.95 |
| $Mg^{2+}$ | 0.97 | 0.98 | 0.99 |
| $Ca^{2+}$ | 0.97 | 0.99 | 1.00 |
| $Cl^-$ | 0.95 | 0.97 | 0.98 |
| $NO_3^-$ | 0.92 | 0.93 | 0.89 |
| $SO_4^{2-}$ | 0.82 | 0.91 | 0.99 |
| nss–$K^+$ | 0.80 | 0.79 | 0.93 |
| nss–$Ca^{2+}$ | 0.96 | 0.99 | 1.00 |
| nss–$SO_4^{2-}$ | 0.82 | 0.91 | 0.98 |

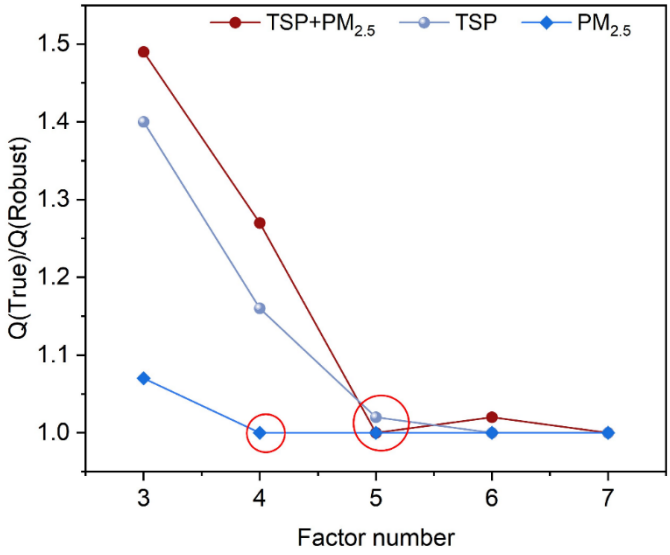


Figure R1. Variation of Q (True)/Q (Robust) with the increase of factor number. The red circles represent the optimal factor number.

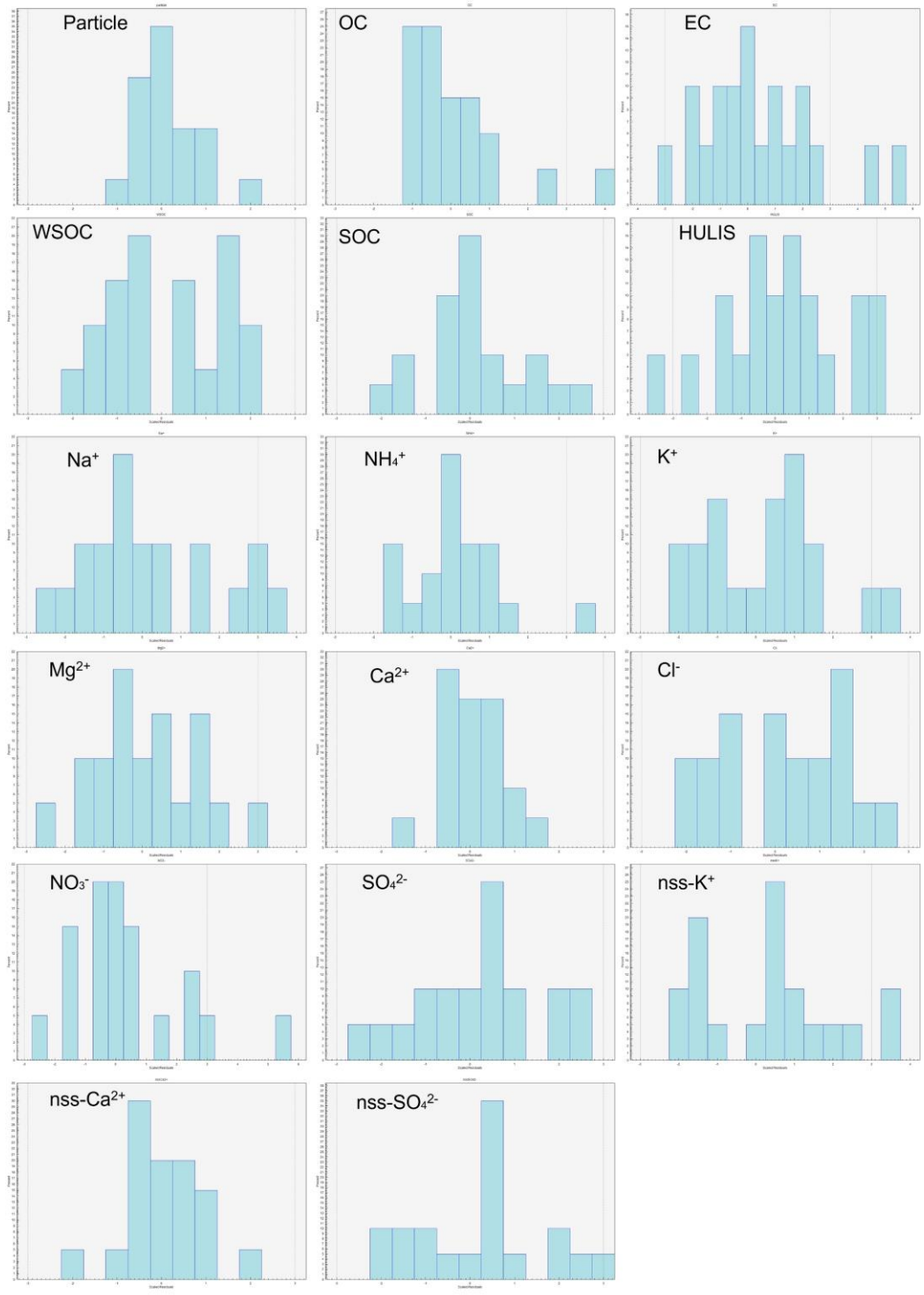


Figure R2. Residual distribution of each species in the five–factor solution.

Given the above error estimation results, it can be proven that the five–factor solution is more robust. Following this, we will mainly discuss the collinearity of the five–factor solution. Our results indicate that the collinearity among the five factors is weak, which

can be demonstrated by the following aspects:

Firstly, DISP results show that there is no factor swap between different factors, and BS results show high factor mapping rates (Table R1). These all suggest that the collinearity between factors is weak.

Secondly, we examined the G–plot between five factors (Figure R3). In theory, when there is no collinearity between factors, sample points should be close to or near the coordinate axis, that is, x = 0 or y = 0. If sample points are far from the coordinate axis or show an approximately correlated straight line, it indicates high collinearity between factors and high rotational uncertainty. Figure R3 shows that for most factors, G–plot shows that most samples points are located near the coordinate axis, indicating that they represent meaningful source contributions rather than redundant or collinear factors. In addition, there is also no significant linear correlation between factors. For mixed sources (combustion source + $SO_4^{2-}$), the G–plot shows that the partial sample points are far away from the coordinate axis. For example, there is a certain linear trend in the G–plot between the mixed source and dust, and partial sample points between the mixed source and the secondary inorganic source are also far away from the coordinate axis. As pointed out by the Referee, terrestrial sources and anthropogenic pollutants occur at the same time. Therefore, the weak collinearity between these three factors may be due to the existence of shared emission zones or atmospheric chemical processes among these sources, such as dust and biomass combustion both coming from land, and $SO_4^{2-}$, $NH_4^-$ and $NO_3^-$ all coming from atmospheric transformation. In summary, our results (DISP, BS, and G-plot) explain that the collinearity of the five–factor solution is relatively weak and acceptable.

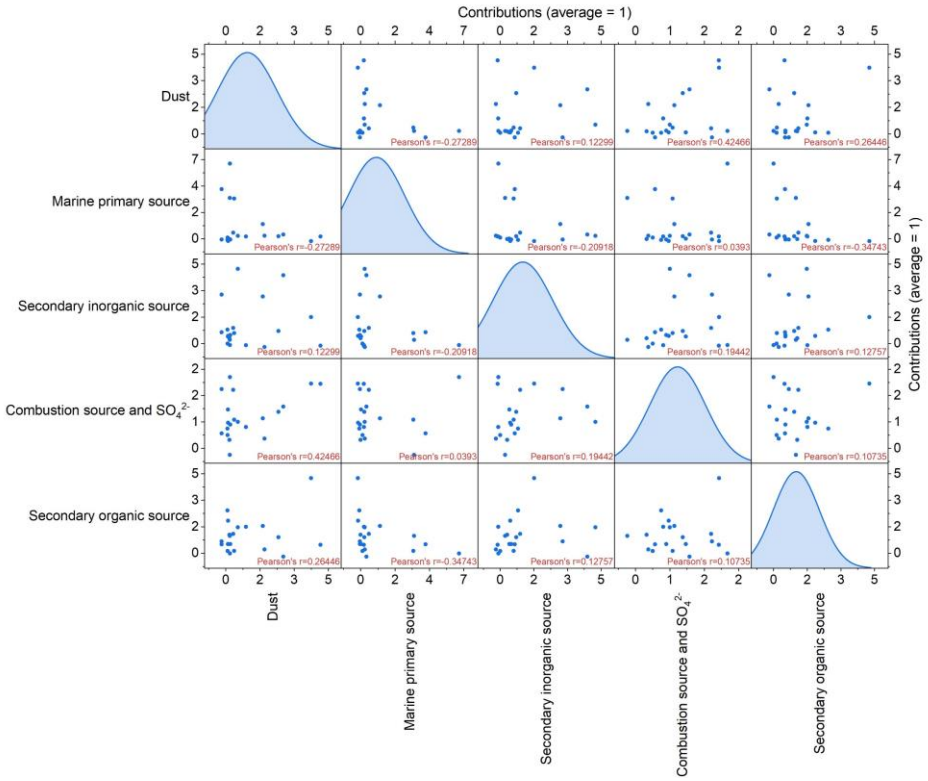


Figure R3. G–plot of five–factor solution.

Based on the Referee's suggestion, before formally discussing the PMF results, we briefly added the following content in the revised manuscript and Supplement to illustrate their robustness.

Main manuscript, Page 14, Line 363–338:

Five factors were identified as the optimal solution. The robustness of PMF results and potential collinearity between factors have been discussed in detail in the Text S3 of the Supplement. Briefly, the five–factor solution has a low Q(True)/Q(Robust) ratio. Two error estimation methods (DISP and BS) jointly reveal that there is no factor swap in five factors, and matching rates of five factors are close to 100%. The scaled residuals of each species are generally within + 3 and - 3, and G–plot reveals a weak collinearity between factors. Therefore, the five–factor solution is relatively robust.

Text S3 of the Supplement, Page 6, Line 112–135:

The collinearity problem between factors is not only affected by the number of factors and the lack of typical tracers, but also by co–emission, co–transport and secondary transformation between sources. The results of DISP and BS jointly reveal that the factor swap does not occur and the factor matching rate is high. This indicates a low

possibility of collinearity caused by the number of factors or tracers. To further evaluate the collinearity caused by co–emission, co–transport and secondary transformation, we compared the G-plots of five factors (Figure S19). In theory, when there is no collinearity between factors, sample points should be close to or near the coordinate axis, that is, x = 0 or y = 0. If sample points are far from the coordinate axis or show an approximately correlated straight line, it indicates high collinearity between factors and high rotational uncertainty. Figure S19 shows that for most factors, G–plot shows that most samples exhibit non–zero or near zero contributions, with many points located near the coordinate axis, indicating that they represent meaningful source contributions rather than redundant or collinear factors. In addition, there is no significant linear correlation between factors. For mixed sources (combustion source + $SO_4^{2-}$), the G–plot shows that the partial sample points are far away from the coordinate axis. For example, there is a certain linear trend in the G–plot between the mixed source and dust, and partial sample points between the mixed source and the secondary inorganic source are also far away from the coordinate axis. The weak collinearity between these three factors may be due to the existence of shared emission zones or atmospheric chemical processes among these sources, such as dust and biomass combustion both coming from land, and $SO_4^{2-}$ $NH_4^-$ and $NO_3^-$ all coming from atmospheric transformation. In summary, our evaluation results (DISP, BS, and G-plot) explain that the collinearity of the five–factor solution is relatively weak and acceptable.

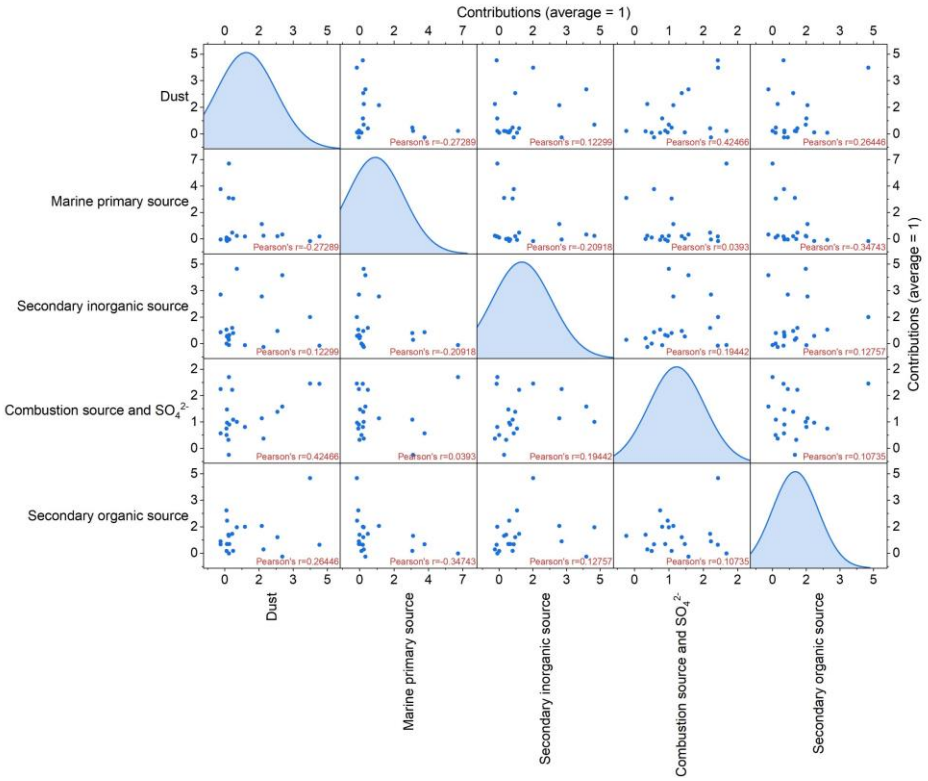


Figure S19. G–plot of five–factor solution.

1. It seems the authors focused on the results of $\delta^{13}C_{TC}$ to analyze the sources of marine organic aerosols. How about the source contributions of marine organic aerosols apportioned by the PMF model? I may suggest to add related discussion in section 3.5.

**Author reply:**

Due to the lack of specific tracers for marine organic aerosols (MOA) in our dataset, PMF was not able to resolve an independent MOA factor. The contribution of marine organic aerosols may be merged into other sources containing OC or SOC, such as secondary organic aerosol source. $\delta^{13}C_{TC}$ provides complementary source information that is less dependent on molecular–level tracers and is particularly useful for distinguishing organic compounds from marine source and combustion–related source. Therefore, when the lack of organic tracers from marine source makes it impossible to analyze the contribution of marine organic aerosols separately through PMF, $\delta^{13}C_{TC}$ can be used as additional evidence to assess the impact of marine organic sources.

We have added a brief discussion in Section 3.5. At the same time, we have adjusted the structure of this section by first introducing the results of PMF, clarifying the limitations of PMF in analyzing the contribution of marine organic aerosol sources in

the absence of marine organic aerosol tracers. Continuing with the introduction of the source apportionment results of $\delta^{13}C_{TC}$, it is clarified that $\delta^{13}C_{TC}$ can serve as a supplement to PMF results, and the potential correlation between the results of $\delta^{13}C_{TC}$ and PMF is briefly explained. The following is the revised content of Section 3.5 (Page 14, Line 362–400) in the revised manuscript:

In order to ensure that the dataset is large enough to generate more reliable results for PMF, we integrated all TSP and $PM_{2.5}$ samples into one dataset, and results are shown in Fig. 4A. Five factors were identified as the optimal solution. The robustness of PMF results and potential collinearity between factors have been discussed in detail in Text S3 of Supplement. Briefly, five–factor solution has a low Q(True)/Q(Robust) ratio. Two error estimation methods (DISP and BS) jointly reveal that there is no factor swap in five factors, and the matching rates of five factors are close to 100%. The scaled residuals of each species are generally within +3 and -3, and G–plot reveals a weak collinearity between factors. Therefore, the five–factor solution is relatively robust.

The species with a high proportion in the profile of factor 1 is $Ca^{2+}$ or nss–$Ca^{2+}$, which is commonly believed to originate from the crust or soil (Stanimirova et al., 2023). This factor is identified as a crustal source. The characteristic ion components in factor 2 are $Na^+$, $Mg^{2+}$ and $Cl^-$, with $Na^+$ and $Cl^-$ exhibiting the highest proportion (Zong et al., 2016). This factor may then be associated with sea salt and is identified as a marine primary source. Factor 3 has a high proportion of secondary inorganic ions ($NH_4^+$ and $NO_3^-$) derived from heterogeneous or homogeneous reaction of $NH_3$ and $NO_2$ (Pathak et al., 2009), and it is considered as a secondary inorganic source (Wei et al., 2024). Factor 4 has high proportions of EC, organic species, nss–$K^+$ and nss–$SO_4^{2-}$. EC and nss–$K^+$ jointly indicate that this factor may have connection with combustion source (biomass burning), while nss–$SO_4^{2-}$ is associated with secondary transformation of $SO_2$ (Dai et al., 2023; Xue et al., 2019). Hence, factor 4 is identified as a mixture source (combustion source and $SO_4^{2-}$). Factor 5, with a high proportion of SOC and low proportions of EC and inorganic species, is considered as a secondary organic source.

The above proportions are consistent with results of previous studies conducted at BS and YS that have also shown that biomass combustion, secondary sources, and sea salt

are common sources of aerosol components (Zhao et al., 2023; Geng et al., 2020; Zhang et al., 2025b). Among them, combustion and secondary sources (secondary organic and inorganic aerosol sources) constituted the largest proportion (> 60%). This highlights the importance of combustion source and atmospheric secondary transformation in the atmosphere of marginal seas. Additionally, the proportion of marine primary sources was relatively low in the northern sea region, while dust and secondary organic aerosol (SOA) sources were higher (Fig. S16), indicating that low Rtbl can still transport significant amounts of terrestrial components.

Due to the lack of typical marine organic tracers, PMF cannot separate the contribution of marine organic aerosol sources alone and can only identify the contribution of marine primary sources. But the $\delta^{13}C_{TC}$ of organic components from terrestrial and marine sources are different. Hence, $\delta^{13}C_{TC}$ can be used as additional evidence to assess the impact of marine organic sources when there is lack of organic tracers in PMF model. The average $\delta^{13}C_{TC}$ value of carbonaceous components in aerosols ranged from –25.9‰ to –24.6‰, with an average of -25.2‰ (–25‰ for TSP, –25.3‰ for $PM_{2.5}$). These values are closer to the characteristic carbon stable isotope signatures of coal combustion and biomass burning aerosols (–24‰ to –28.4‰) and lower than those of typical marine sources (–18‰ to –23‰) (Bikkina et al., 2022; Crocker et al., 2020). Combining above results with a Bayesian mixing model, we found that carbonaceous components in BS and YS summer aerosols were predominantly influenced by biomass burning sources, primarily from C3 plant burning, contributing approximately 60–80% to the carbonaceous fraction. Biomass burning remained dominant even when accounting for isotopic fractionation effects (Fig. 4B–E). The high contribution of biomass burning may have connection with dense open fire points in coastal terrestrial regions. In general, marine emission only contribute less than 10% of carbonaceous species. However, due to the different principles of the two models, it is difficult to match the $\delta^{13}C_{TC}$ results with the PMF results. Nevertheless, it can be speculated that in the PMF model, the contribution of marine emissions to organic aerosols may be merged into other sources containing OC or SOC, such as secondary organic aerosol source. In the future, it is necessary to include typical marine organic tracers (such as

methanesulfonic acid) to the PMF model for more accurate source apportionment.

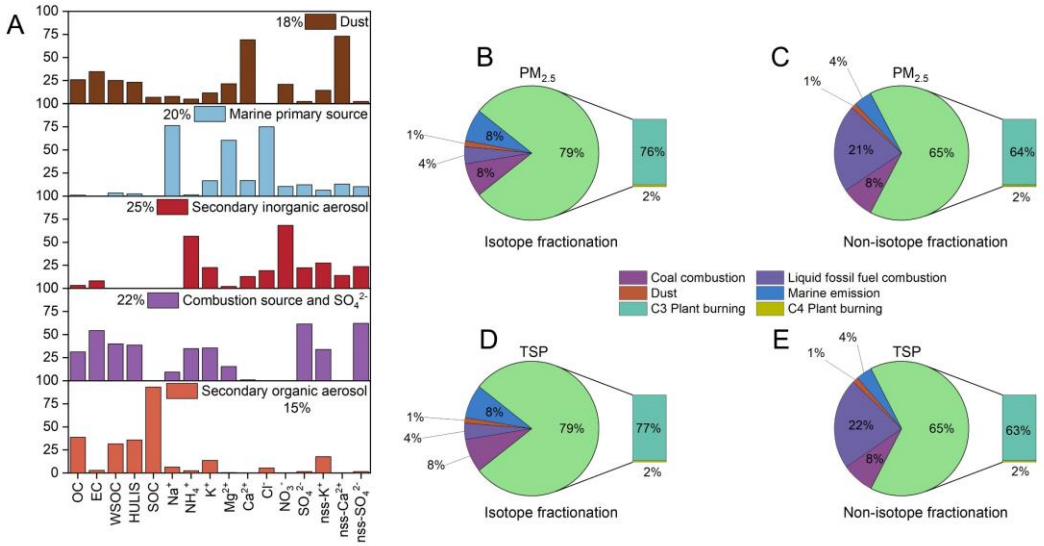


**Figure 4. (A) Source apportionment based on PMF. (B) to (E) Source apportionment based on $\delta^{13}C_{TC}$.**

2. This work highlights the importance of coastal emissions on the marine aerosols over the marginal seas. What do you mean "coastal emissions" here? It is unclear. Please specific in the title and throughout the manuscript. The "properties" in the title is unclear. Pleas be specific.

**Author reply:**

We have revised the title and the entire manuscript regarding the expression of coastal emissions and properties. The description of coastal emissions in the entire manuscript has been revised to coastal terrestrial emissions.

Revised title: Coastal terrestrial emissions modify the composition and optical properties of aerosols in marginal seas

Further corrections in the revised manuscript.

Page 2, Line 51: Marginal seas are adjacent to coastal terrestrial regions with important human activities and high anthropogenic emissions.

Page 8, Line 197: The orange region represents the coastal terrestrial regions of China.

Page 11, Line 279: The precursors of these biogenic SOA are most likely isoprene and monoterpenes released by terrestrial plants in coastal terrestrial regions and

phytoplankton in coastal waters.

Page 12, Line 324: Therefore, anthropogenic pollutants can enter BS and YS through rivers in coastal terrestrial regions and reenter the atmosphere via sea spray.

Page 14, Line 359: This indicates that coastal terrestrial regions are the most likely sources of summer BS and YS aerosols.

Page 14, Line 360: Hence, we speculate that components in aerosols over BS and YS are more likely to originate from coastal terrestrial regions rather than inland.

Page 16, Line 425: From a global perspective, coastal terrestrial regions (usually within 100 km of the coastline) accommodate nearly one-third of the global population with a relatively small land area (18%), contribute nearly 82% of the world's gross domestic product (GDP) and contain 67% of mega cities.

Page 16, Line 429: Therefore, even in winter and spring seasons, anthropogenic emissions from coastal terrestrial regions should be dominant for the atmospheric environment of marginal seas.

Page 16, Line 431–432: Our results emphasize the importance of coastal terrestrial emissions in controlling marginal sea environmental pollution by quantifying the range of coastal terrestrial regions that affect the atmospheric environment of BS and YS.

Page 16, Line 432–433: Controlling coastal terrestrial emissions is an important measure to alleviate marginal sea environmental pollution.

Page 16, Line 435–437: At the same time, it also suggests that when using regional climate chemistry coupling models to simulate land–sea interactions, special attention should be paid to updating coastal terrestrial emissions.

3. The abbreviations (e.g., Rmbl, Rtbl, Rmam, Rtam) in Fig 1b are not easy to follow. And similar abbreviations appear a lot in the main text. I may suggest to use more concise and clear abbreviations throughout the manuscript, and define them clearly when they first appear.

**Author reply:**

The meanings of these four letters are:

R stands for Retention ratio

mbl stands for marine boundary layer

tbl stands for terrestrial boundary layer

mam stands for marine air masses

tam stands for terrestrial air masses

Full names of these abbreviations are provided in Section 2.4 and in the caption of Figure 1 in the revised manuscript. The specific modifications are as follows:

Page 5, Line 131: The retention ratios of terrestrial air masses (Rtam) and marine air masses (Rmam) are calculated and modified from the method proposed by previous studies.

Page 6, Line 146–147: Rtbl indicates the retention ratio of terrestrial boundary layer air mass. Rmbl indicates the retention ratio of marine boundary layer air mass.

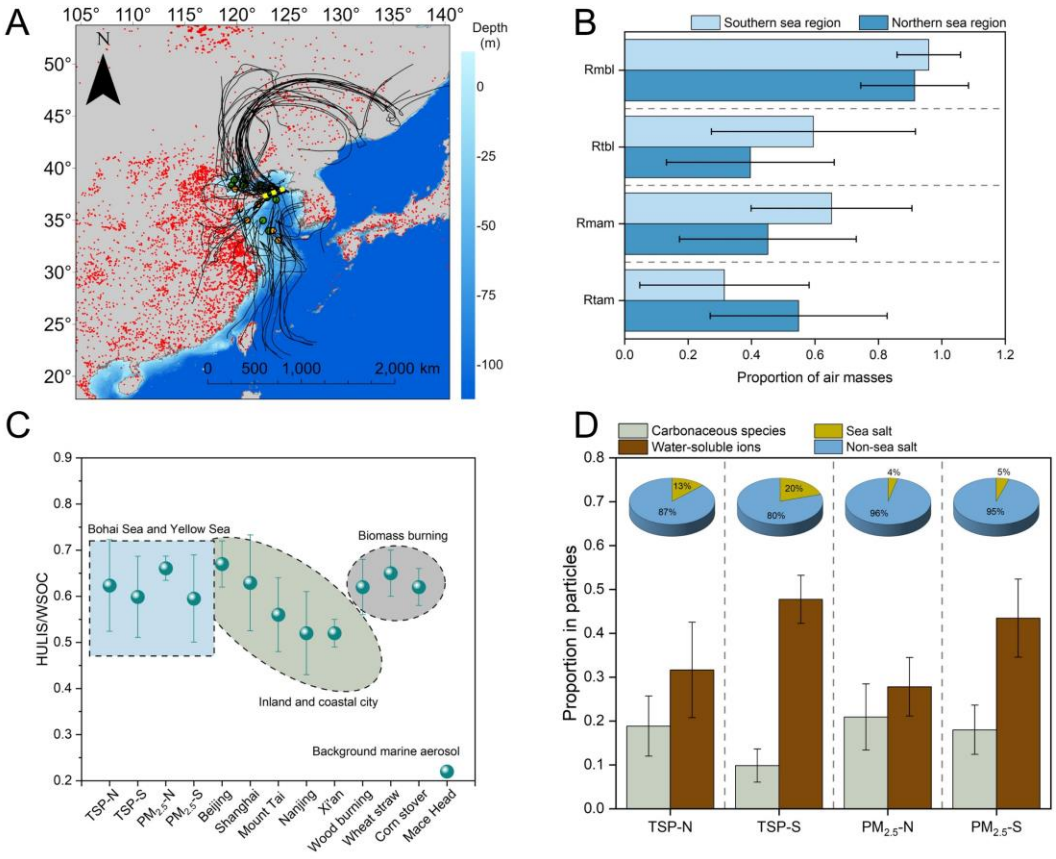


**Figure 1. (A) Trajectories of air masses arriving at the Yellow Sea and Bohai Sea during the sampling period. The simulated air mass transport time is 72 h. Green, yellow and red points represent TSP, $PM_{2.5}$ samples and fire points, respectively. Fire point information comes from https://firms.modaps.eosdis.nasa.gov/map. The yellow dashed line represents the boundary between the northern and southern sea regions. (B) Retention ratio of air masses over land and ocean, as well as the retention ratio of boundary layer air masses. Rmbl**

**stands for Retention ratio of marine boundary layer air masses, Rtbl stands for Retention ratio of terrestrial boundary layer air masses, Rmam stands for Retention ratio of marine air masses and Rtam stands for Retention ratio of terrestrial air masses. (C) Differences in HULIS/WSOC ratio at different sampling points. (D) Proportion of carbonaceous species and water–soluble ions in particles. The pie charts represent the proportion of sea salt ions and non–sea salt ions in the total ions of each sea region. N and S indicate the northern and southern sea regions, respectively.**

4. Lines 186-187: Please explain this statement in detail. Do you have any related references?

**Author reply:**

Our original idea was to express that air masses flowing over the ocean spend more than 90% of their time within the boundary layer, while air masses flowing over land spend less than 60% of their time in the boundary layer (Figure 1B). Hence, the retention ratio of terrestrial boundary layer air masses (Rtbl) reaching both sea regions is lower than that of marine boundary layer air masses (Rmbl). Considering that atmospheric pollutants mainly constrained within the boundary layer, high Rmbl theoretically indicates that aerosols are more affected by marine emissions. Previous studies have used these two parameters to evaluate the impact of air mass transport on the atmosphere of the Yellow Sea, East China Sea, and Gulf of Aqaba (Zhou et al., 2023; Zhou et al., 2021; Yan et al., 2024).

We have rewritten the related sentence and added more references as follows:

Page 8, Line 199–202:

During the sampling period, we observed that the retention ratio of marine boundary layer air masses (Rmbl) in the two sea regions (> 90%) was higher than that of terrestrial boundary layer air masses (Rtbl) (< 60%) (Fig. 1B). Considering that atmospheric pollutants mainly constrained within the boundary layer, high Rmbl theoretically indicates that aerosols are more affected by marine emissions (Zhou et al., 2023; Zhou et al., 2021; Yan et al., 2024).

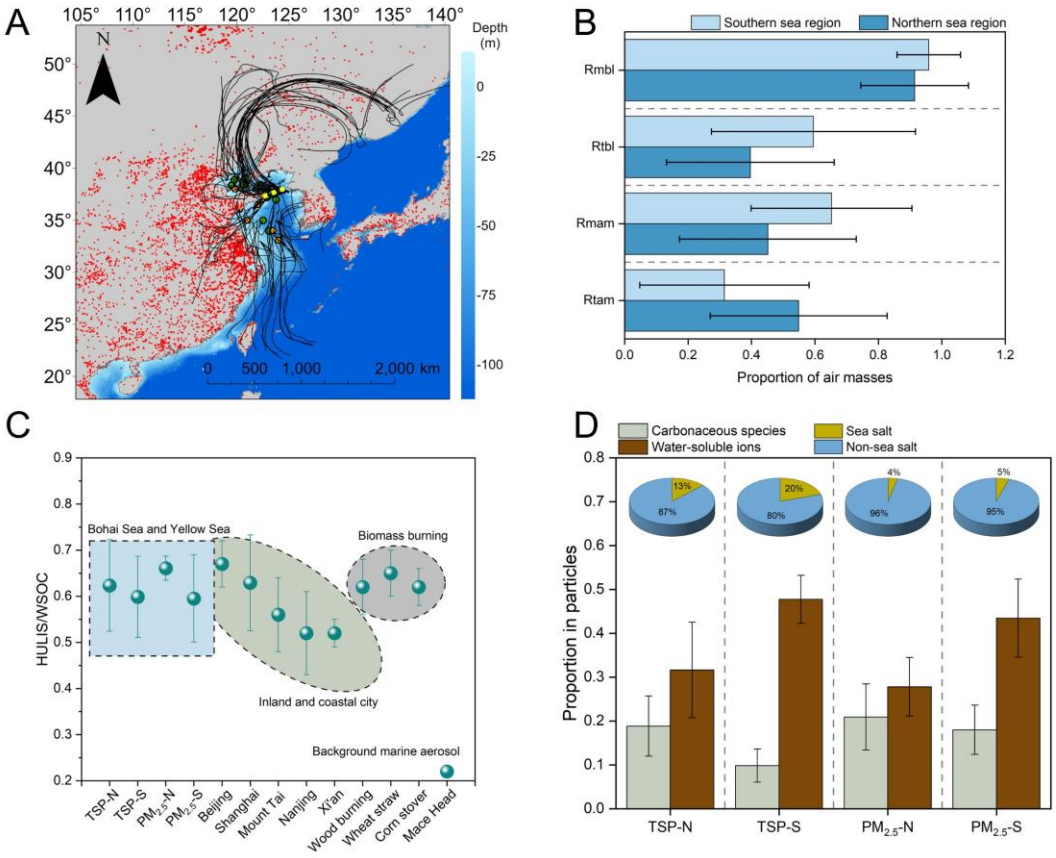


**Figure 1. (A) Trajectories of air masses arriving at the Yellow Sea and Bohai Sea during the sampling period. The simulated air mass transport time is 72 hours. Green, yellow and red points represent TSP, $PM_{2.5}$ samples and fire points, respectively. Fire point information comes from https://firms.modaps.eosdis.nasa.gov/map. The yellow dashed line represents the boundary between the northern and southern sea regions. (B) Retention ratio of air masses over land and ocean, as well as the retention ratio of boundary layer air masses. Rmbl stands for Retention ratio of marine boundary layer air masses, Rtbl stands for Retention ratio of terrestrial boundary layer air masses, Rmam stands for Retention ratio of marine air masses and Rtam stands for Retention ratio of terrestrial air masses. (C) Differences in HULIS/WSOC ratio at different sampling points. (D) Proportion of carbonaceous species and water–soluble ions in particles. The pie charts represent the proportion of sea salt ions and non–sea salt ions in the total ions of each sea region. N and S indicate the northern and southern sea regions, respectively.**

5. Lines 310-311: What do you mean "no significant differences in...." here? Please explain and be specific.

**Author reply:**

The term “no significant differences” here was used to express the fact that the optical parameters ($Abs_{365}$ and $MAE_{365}$) of the light–absorbing components (WSOC, HULIS, WISOC) in aerosols do not differ significantly between the northern and southern sea

regions, just as shown in Table R5 below. To make it clear, we have revised the sentence as follows:

Page 12, Line 331–332

Our results show that there is no apparent difference in the light–absorbing parameters ($Abs_{365}$ and $MAE_{365}$) of typical light–absorbing components between the two sea regions (Table S5).

Table R5. Major light absorption parameters of TSP and $PM_{2.5}$ in the two sea regions.

| | TSP | | | $PM_{2.5}$ | | |
|---|---|---|---|---|---|---|
| | $Abs_{365}$ ($Mm^{-1}$) | $MAE_{365}$ ($m^2\ g^{-1}$) | AAE | $Abs_{365}$ ($Mm^{-1}$) | $MAE_{365}$ ($m^2\ g^{-1}$) | AAE |
| WSOC North | 1.20 ± 0.68 | 0.26 ± 0.05 | 6.68 ± 0.52 | 0.54 ± 0.13 | 0.22 ± 0.02 | 7.01 ± 0.08 |
| WSOC South | 1.01 ± 0.42 | 0.25 ± 0.08 | 6.98 ± 0.69 | 0.75 ± 0.49 | 0.22 ± 0.09 | 6.74 ± 0.31 |
| HULIS North | 0.79 ± 0.46 | 0.27 ± 0.03 | 7.56 ± 0.73 | 0.46 ± 0.12 | 0.28 ± 0.02 | 7.40 ± 0.17 |
| HULIS South | 0.54 ± 0.30 | 0.29 ± 0.05 | 7.55 ± 0.77 | 0.51 ± 0.32 | 0.24 ± 0.09 | 7.41 ± 0.35 |
| WISOC North | 0.73 ± 0.38 | 0.13 ± 0.03 | 6.34 ± 0.79 | 0.29 ± 0.12 | 0.12 ± 0.07 | 5.56 ± 0.62 |
| WISOC South | 0.52 ± 0.18 | 0.20 ± 0.09 | 6.16 ± 0.76 | 0.30 ± 0.15 | 0.13 ± 0.03 | 5.97 ± 1.26 |

## References


Bikkina, P., Bikkina, S., Kawamura, K., Sarma, V., and Deshmukh, D. K.: Unraveling the sources of atmospheric organic aerosols over the Arabian Sea: Insights from the stable carbon and nitrogen isotopic composition, Sci. Total Environ., 827, 154260, https://doi.org/10.1016/j.scitotenv.2022.154260, 2022.

Crocker, D. R., Hernandez, R. E., Huang, H. D., Pendergraft, M. A., Cao, R., Dai, J., Morris, C. K., Deane, G. B., Prather, K. A., and Thiemens, M. H.: Biological Influence on δ13C and Organic Composition of Nascent Sea Spray Aerosol, ACS Earth Space Chem., 4, 1686–1699, https://doi.org/10.1021/acsearthspacechem.0c00072, 2020.

Dai, Q., Chen, J., Wang, X., Dai, T., Tian, Y., Bi, X., Shi, G., Wu, J., Liu, B., Zhang, Y., Yan, B., Kinney, P. L., Feng, Y., and Hopke, P. K.: Trends of source apportioned $PM_{2.5}$ in Tianjin over 2013–2019: Impacts of Clean Air Actions, Environ. Pollut., 325, 121344, https://doi.org/10.1016/j.envpol.2023.121344, 2023.

Geng, X., Mo, Y., Li, J., Zhong, G., Tang, J., Jiang, H., Ding, X., Malik, R. N., and Zhang, G.: Source apportionment of water-soluble brown carbon in aerosols over the northern South China Sea: Influence from land outflow, SOA formation and marine emission, Atmos. Environ.,

229, 117484, https://doi.org/10.1016/j.atmosenv.2020.117484, 2020.

Song, M., Tan, Q., Feng, M., Qu, Y., Liu, X., An, J., and Zhang, Y.: Source Apportionment and Secondary Transformation of Atmospheric Nonmethane Hydrocarbons in Chengdu, Southwest China, J. Geophys. Res.-Atmos., 123, 9741–9763, https://doi.org/10.1029/2018jd028479, 2018b.

Pathak, R. K., Wu, W. S., and Wang, T.: Summertime $PM_{2.5}$ ionic species in four major cities of China: nitrate formation in an ammonia-deficient atmosphere, Atmos. Chem. Phys., 9, 1711–1722, https://doi.org/10.5194/acp-9-1711-2009, 2009.

Stanimirova, I., Rich, D. Q., Russell, A. G., and Hopke, P. K.: A long-term, dispersion normalized PMF source apportionment of $PM_{2.5}$ in Atlanta from 2005 to 2019, Atmos. Environ., 312, 120027, https://doi.org/10.1016/j.atmosenv.2023.120027, 2023.

Wei, Y., Wang, S., Jiang, N., Zhang, D., and Zhang, R.: Study on main sources of aerosol pH and new methods for additional reduction of $PM_{2.5}$ during winter severe pollution: Based on the PMF-GAS model, J. Clean Prod., 471, 143401, https://doi.org/10.1016/j.jclepro.2024.143401, 2024.

Xue, J., Yu, X., Yuan, Z., Griffith, S. M., Lau, A. K. H., Seinfeld, J. H., and Yu, J. Z.: Efficient control of atmospheric sulfate production based on three formation regimes, Nat. Geosci., 12, 977–982, https://doi.org/10.1038/s41561-019-0485-5, 2019.

Yan, S. B., Xu, G. B., Zhang, H. H., Wang, J., Xu, F., Gao, X. X., Zhang, J. W., Wu, J. W., and Yang, G. P.: Factors Controlling DMS Emission and Atmospheric Sulfate Aerosols in the Western Pacific Continental Sea, J. Geophys. Res.-Oceans., 129, e2024JC020886, https://doi.org/10.1029/2024jc020886, 2024.

Zhang, Y., Wang, Y., Li, S., Yi, Y., Guo, Y., Yu, C., Jiang, Y., Ni, Y., Hu, W., Zhu, J., Qi, J., Shi, J., Yao, X., and Gao, H.: Sources and Optical Properties of Marine Organic Aerosols Under the Influence of Marine Emissions, Asian Dust, and Anthropogenic Pollutants, J. Geophys. Res.-Atmos., 130, e2025JD043472, https://doi.org/10.1029/2025jd043472, 2025b.

Zhao, S., Qi, J., and Ding, X.: Characteristics, seasonal variations, and dry deposition fluxes of carbonaceous and water-soluble organic components in atmospheric aerosols over China's marginal seas, Mar. Pollut. Bull., 191, 114940, https://doi.org/10.1016/j.marpolbul.2023.114940, 2023.

Zhou, S., Chen, Y., Wang, F., Bao, Y., Ding, X., and Xu, Z.: Assessing the Intensity of Marine Biogenic Influence on the Lower Atmosphere: An Insight into the Distribution of Marine Biogenic Aerosols over the Eastern China Seas, Environ. Sci. Technol., 57, 12741–12751, https://doi.org/10.1021/acs.est.3c04382, 2023.

Zhou, S., Chen, Y., Paytan, A., Li, H., Wang, F., Zhu, Y., Yang, T., Zhang, Y., and Zhang, R.: Non-Marine Sources Contribute to Aerosol Methanesulfonate Over Coastal Seas, J. Geophys. Res.-Atmos., 126, e2021JD034960, https://doi.org/10.1029/2021jd034960, 2021.

Zong, Z., Wang, X., Tian, C., Chen, Y., Qu, L., Ji, L., Zhi, G., Li, J., and Zhang, G.: Source apportionment of $PM_{2.5}$ at a regional background site in North China using PMF linked with radiocarbon analysis: insight into the contribution of biomass burning, Atmos. Chem. Phys., 16, 11249–11265, https://doi.org/10.5194/acp-16-11249-2016, 2016.